A First Order Vorticity Equation for Tropical Easterly Waves

HAN-RU CHO, MARY ANN JENKINS AND JOSEPH BOYD

Department of Physics, University of Toronto, Toronto, Ontario, Canada M5S 1A7

(Manuscript received 20 September 1982, in final form 6 December 1982)

ABSTRACT

A first order vorticity equation for tropical disturbances is derived. The equation indicates that the evolution of the vorticity field in the tropical atmosphere is influenced mainly by the horizontal advection of vorticity, and a vorticity source produced by cumulus convection.

The A/B-scale vorticity budgets during Phase III of the GARP Atlantic Tropical Experiment (GATE) are analyzed to provide a consistency check between the first order vorticity equation and observations. The results show that the equation agrees well with the observed evolution of the large-scale vorticity field, at least in the diagnostic sense.

The simple vorticity equation is also used to study the vorticity dynamics of tropical easterly waves observed in GATE; certain features of the vorticity and divergence fields are related through the first order vorticity equation. In particular, the pronounced mid-level divergence often observed in GATE during convectively active periods is found to be associated with the vorticity advection by the west African easterly jet at the 650 mb level.

1. Introduction

It is well known that cumulus convection strongly influences the structure of tropical disturbances. But because cloud-mean-flow interactions are very complex, the relationships between the collective effects of cumulus clouds and the observed structures of tropical disturbances are not yet understood. Many unsolved problems still remain.

Discovering the processes responsible for the thermal structure of tropical easterly waves is a typical example of one of the problems. Using the composite technique, Reed and Recker (1971) and Thompson *et al.* (1979) obtained temperature fields for tropical easterly waves over the western Pacific and eastern Atlantic, respectively. Presumably, cumulus heating is responsible for the thermal structure of these fields. Many studies were done to understand the processes by which the latent heat released inside cumulus clouds may be imparted to the large scale flow (Ooyama, 1971; Fraedrich, 1973; Yanai *et al.*, 1973; Arakawa and Schubert, 1974; Nitta, 1975; Johnson, 1976; Cho, 1977). Yet, it is still unknown how cumulus heating leads to the observed thermal structure.

There are similar problems for the momentum fields of tropical disturbances. A few theories of the effects of cumulus convection on the larger scale vorticity field were developed during the past several years (Shapiro, 1978; Cho *et al.*, 1979; Cho and Cheng, 1980; Shapiro and Stevens, 1980; Yanai *et al.*, 1982). According to these theories, clouds may modify the large-scale vorticity field by several processes. Diagnostic studies using GARP Atlantic Tropical Experiment (GATE) data indicate that the relative importance of the processes varies from case to case (Shapiro, 1978; Shapiro and Stevens, 1980; Cho and Cheng, 1980; Jenkins *et al.*, 1982). The net effect is often a delicate balance between these processes; it shows a rather complex vertical structure which cannot be easily interpreted in simple terms. To understand the behavior of tropical disturbances, better physical insights into the interaction between cumulus cloud and the larger scale flow are needed.

The purpose of this paper is to discuss a systematic method that is used to simplify the vorticity equation for the tropical atmosphere. We hope to identify the first order effect of cumulus convection and to explain how the large-scale vorticity field may evolve in response to cloud forcing. The parameterization scheme introduced by Cho and Cheng (1980) is used to represent the collective effect of cumulus clouds on the large-scale vorticity field. Because the simplification introduced to the complete vorticity equation is based on a condition derived from thermodynamic considerations, a brief discussion of the thermodynamic equation is presented in Section 2. The formal derivation of the first order vorticity equation is given in Section 3, followed by some supporting observational evidence derived from the GATE data in Section 4. The implications of the simple vorticity equation for tropical easterly waves are discussed in Section 5. The paper is concluded by a few additional remarks in Section 6.

2. The thermodynamic equation

Using the potential temperature θ, the first law of thermodynamics for the mean flow can be written as

$$\frac{\partial\bar{\theta}}{\partial t} + \bar{\mathbf{v}}\cdot\nabla\bar{\theta} + \bar{\omega}\frac{\partial\bar{\theta}}{\partial p} = -M_c\frac{\partial\bar{\theta}}{\partial p}. \tag{1}$$

The overbar denotes the horizontal areal average which is used to separate the mean flow from the cloud-scale motion. The cloud effect is represented on the right-hand side of the equation in terms of the total cloud mass flux M_c. This is the representation first proposed by Ooyama (1971) and Arakawa and Schubert (1974) and later refined by Cho (1977). In Cho's formulation, cloud areas are defined as regions where condensation and evaporation processes take place. Consequently, M_c includes both the condensation-induced upward motion and evaporation-induced cloud-scale downward motion.

It is well known from observations that the temperature variations in synoptic-scale tropical disturbances are very small. The horizontal total derivative of potential temperature is only of the order of 0.3°C day^{-1}:

$$\frac{\partial\bar{\theta}}{\partial t} + \bar{\mathbf{v}}\cdot\nabla\bar{\theta} \approx 0.3°\text{C day}^{-1}. \tag{2}$$

The heating rate due to cumulus clouds in convectively active regions of these disturbances is considerably larger, typically of the order

$$-M_c\frac{\partial\bar{\theta}}{\partial p} \approx 10°\text{C day}^{-1}. \tag{3}$$

As noted by Wallace (1971), this implies that the cloud heating is balanced mainly by the adiabatic cooling associated with the large-scale ascending motion. As a zeroth order approximation, (1) may be reduced to

$$\bar{\omega}\frac{\partial\bar{\theta}}{\partial p} = -M_c\frac{\partial\bar{\theta}}{\partial p}, \tag{4}$$

or

$$\bar{\omega} = -M_c. \tag{5}$$

The large-scale mean ascending motion in the core regions of these disturbances is essentially equal to the total upward mass flux induced inside cumulus clouds. Consequently, the mean vertical motion in the cloud environment, given by

$$\tilde{\omega} = \bar{\omega} + M_c, \tag{6}$$

must be very weak. It is usually a small difference between two large quantities $\bar{\omega}$ and M_c.

It should be noted that, as a zeroth order approximation, (4) and (5) are valid only in regions where cloud activities are reasonably strong. The degree of approximation is measured by the parameter

$$r = \frac{\left|\dfrac{\partial\bar{\theta}}{\partial t} + \bar{\mathbf{v}}\cdot\nabla\bar{\theta}\right|}{\left|M_c\dfrac{\partial\bar{\theta}}{\partial p}\right|}. \tag{7}$$

The zeroth order approximation may be applied only if $r \ll 10^{-1}$, which is the case in most tropical disturbances.

However, the conclusion that the vertical velocity in the cloud environment $\tilde{\omega}$ is very weak is valid, independent of the strength of cumulus convection. This can be shown by writing the thermodynamic Eq. (1) in terms of $\tilde{\omega}$, following the approach adopted by Ooyama (1971),

$$\frac{\partial\bar{\theta}}{\partial t} + \bar{\mathbf{v}}\cdot\nabla\bar{\theta} + \tilde{\omega}\frac{\partial\bar{\theta}}{\partial p} = 0. \tag{8}$$

In addition to the horizontal thermal advection, the mean temperature field is influenced by the vertical motion in the cloud environment. The portion of latent heat released inside cumulus clouds that may be imparted to the mean flow depends on the ability of the clouds to influence the vertical motion field in the cloud environment. From (2) and (8), the typical values of $\tilde{\omega}$ should be of the order 0.3°C day^{-1}/$(\partial\bar{\theta}/\partial p)$, which is very small.

This conclusion can also be derived from a scale analysis. Assuming that the pressure gradient force is comparable in magnitude to the Coriolis force, the fractional change of potential temperature has a typical magnitude given by the ratio of the Froude number (Fr) to the Rossby number (Ro):

$$\frac{\Delta\theta}{\theta} \approx \frac{\text{Fr}}{\text{Ro}}, \tag{9}$$

where Ro = V/fL and Fr = V^2/gD. In these expressions, V is the horizontal velocity scale, L and D are the horizontal and vertical length scales of the disturbance, f the Coriolis parameter and g is the gravitational acceleration. The magnitude of $\tilde{\omega}$ may then be estimated from (8) as

$$\tilde{\omega} \approx P(V/L)(\text{Fr}/\text{Ro})/S, \tag{10}$$

where P is the vertical pressure scale, and $S = (P/\bar{\theta})(\partial\bar{\theta}/\partial p)$ is a static stability parameter. For synoptic scale disturbances in the tropical latitudes, Ro ≈ 1, Fr $\approx 10^{-3}$, and $S \approx 10^{-1}$. From (10), the magnitude of the mean divergence in the cloud environment can be estimated:

$$\tilde{\omega}/P \approx (V/L)(\text{Fr}/\text{Ro})/S \approx 10^{-2}(V/L). \tag{11}$$

It is approximately two orders smaller than the magnitude of the vorticity. This estimate together with Eq. (8) are valid, independent of the strength of cloud activities. They are applicable to cloud free areas as well, in which case $M_c = 0$ and $\tilde{\omega} = \bar{\omega}$.

So far in this analysis we have ignored the effect of radiative heating Q_R. It may be reintroduced by defining a radiation-induced vertical motion field $\bar{\omega}_R$ according to

$$\bar{\omega}_R \frac{\partial \bar{\theta}}{\partial p} = Q_R. \tag{12}$$

At the zeroth order, the thermodynamic equation is reduced to

$$\bar{\omega} + \bar{\omega}_R = -M_c. \tag{13}$$

The complete thermodynamic equation can be written as

$$\frac{\partial \bar{\theta}}{\partial t} + \bar{\mathbf{v}} \cdot \nabla \bar{\theta} + (\tilde{\omega} + \bar{\omega}_R) \frac{\partial \bar{\theta}}{\partial p} = 0. \tag{14}$$

The typical values of the radiative heating rate Q_R are of the order of -1 to -2°C day^{-1} and are smaller than the observed cumulus heating rate by about a factor of five in most tropical disturbances. Therefore, for simplicity's sake, we ignore the effects of radiation in our analysis.

3. The first order vorticity equation

We shall demonstrate in this section how the complete vorticity equation may be simplified using the result of the previous section that the vertical motion in the cloud environment is very weak.

The large-scale mean vertical vorticity equation, including the effects of cumulus clouds, can be written as

$$\frac{\partial \bar{\eta}}{\partial t} + \bar{\mathbf{v}} \cdot \nabla \bar{\eta} + \bar{\eta} \nabla \cdot \bar{\mathbf{v}} + \bar{\omega} \frac{\partial \bar{\eta}}{\partial p} + \hat{\mathbf{k}} \cdot \nabla \bar{\omega} \times \frac{\partial \bar{\mathbf{v}}}{\partial p}$$
$$= -\nabla \cdot \overline{\mathbf{v}'\eta'} - \overline{\omega' \frac{\partial \eta'}{\partial p}} - \hat{\mathbf{k}} \cdot \overline{\nabla \omega' \times \frac{\partial \mathbf{v}'}{\partial p}} \tag{15}$$

where η is the vertical component of absolute vorticity, and $\hat{\mathbf{k}}$ the unit vector in the vertical direction. The effect of the cumulus clouds is described by the terms of the right-side of (15). It is usually referred to as the apparent vorticity source Z, where

$$Z = -\nabla \cdot \overline{\mathbf{v}'\eta'} - \overline{\omega' \frac{\partial \eta'}{\partial p}} - \hat{\mathbf{k}} \cdot \overline{\nabla \omega' \times \frac{\partial \mathbf{v}'}{\partial p}}. \tag{16}$$

In this analysis, the formulation proposed by Cho and Cheng (1980) will be used to parameterize the effect of cumulus clouds on the large-scale vorticity field. According to these authors, the apparent vorticity source is given by

$$Z = \left(\int \frac{\sigma}{\tau} dp'\right)(\bar{\eta}_c - \bar{\eta}) + \bar{\eta} \frac{\partial M_c}{\partial p}$$
$$- M_c \frac{\partial \bar{\eta}}{\partial p} - \hat{\mathbf{k}} \cdot \nabla M_c \times \frac{\partial \bar{\mathbf{v}}}{\partial p}. \tag{17}$$

It is expressed in terms of the total cloud mass flux M_c, the atmospheric recycling rate by cumulus clouds $\left(\int \frac{\sigma}{\tau} dp'\right)$, and the ensemble mean cloud vorticity $\bar{\eta}_c$.

Results of observational studies indicate that the mean absolute vorticity $\bar{\eta}$ and mean divergence $\bar{\delta}$ in synoptic scale tropical disturbances are of the same order in magnitude:

$$\bar{\eta}, \bar{\delta} \approx \frac{V}{L} \approx 10^{-5}\ \text{s}^{-1}.$$

This means that all the terms in the mean vorticity equation, (15) and (17), have magnitude comparable to $(V/L)^2$. Studies done by Shapiro and Stevens (1980), Chu *et al.* (1981), and Jenkins *et al.* (1982) show that the vertical advection and tilting of vorticity by the mean vertical motion field are usually somewhat smaller than the other terms in the mean vorticity equation. But in general they are not negligible. No single term in the complete vorticity equation can be neglected.

A systematic simplification of the vorticity equation is achieved by noting that for every term involving the mean vertical motion $\bar{\omega}$ on the left side of (15), there is a corresponding term representing the cloud effect involving the total cloud mass flux M_c on the right side of the equation. Since the zeroth order thermodynamic equation implies that $\bar{\omega} = -M_c$, these terms essentially cancel one another. Formally, using (6), we combine the terms in the mean vorticity equation involving $\bar{\omega}$ and M_c and write the equation in terms of the vertical velocity in the cloud environment $\tilde{\omega}$ as

$$\frac{\partial \bar{\eta}}{\partial t} + \bar{\mathbf{v}} \cdot \nabla \bar{\eta} = \left(\int \frac{\sigma}{\tau} dp'\right)(\bar{\eta}_c - \bar{\eta})$$
$$+ \bar{\eta} \frac{\partial \tilde{\omega}}{\partial p} - \tilde{\omega} \frac{\partial \bar{\eta}}{\partial p} - \hat{\mathbf{k}} \cdot \nabla \tilde{\omega} \times \frac{\partial \bar{\mathbf{v}}}{\partial p}. \tag{18}$$

The magnitude of the left side terms may be estimated as

$$\frac{\partial \bar{\eta}}{\partial t} + \bar{\mathbf{v}} \cdot \nabla \bar{\eta} \approx \left(\frac{V}{L}\right)^2.$$

Since according to (10) $\tilde{\omega} \approx (PV\,\text{Fr}/L\text{Ro}S)$, the last three terms in (18) have magnitudes given by

$$\bar{\eta} \frac{\partial \tilde{\omega}}{\partial p}, \tilde{\omega} \frac{\partial \bar{\eta}}{\partial p}, \hat{\mathbf{k}} \cdot \nabla \tilde{\omega} \times \frac{\partial \bar{\mathbf{v}}}{\partial p} \approx \left(\frac{V}{L}\right)^2 \frac{\text{Fr}}{\text{Ro}} \frac{1}{S} \approx 10^{-2}\left(\frac{V}{L}\right)^2.$$

They are relatively small. The magnitude of the term representing the cloud life-cycle effect may be estimated by assuming (see, e.g., Cheng *et al.*, 1980) that

$$(\bar{\eta}_c - \bar{\eta}) \approx \bar{\eta} \approx \left(\frac{V}{L}\right).$$

Since the recycling rate has a magnitude

$$\int \frac{\sigma}{\tau}\, dp' \approx \frac{\Sigma}{\tau},$$

where Σ is the fractional cloud coverage and τ the mean cloud life span, the magnitude of the first term on the right side of (18) is estimated as

$$\int \frac{\sigma}{\tau}\, dp'(\bar{\eta}_c - \bar{\eta}) \approx \frac{\Sigma}{\tau}\,\bar{\eta} \approx \frac{\Sigma}{\tau}\left(\frac{V}{L}\right).$$

This is comparable to the horizontal advection of vorticity if Σ is of the order of a few per cent and τ is O(1 h). Consequently, as a first order approximation, the vorticity equation can be simplified to obtain

$$\frac{\partial \bar{\eta}}{\partial t} + \bar{\mathbf{v}} \cdot \nabla \bar{\eta} = \left(\int \frac{\sigma}{\tau}\, dp'\right)(\bar{\eta}_c - \bar{\eta}). \qquad (19)$$

The approximation is to the first order of Fr/(RoS).

Eq. (19), the simplified vorticity equation, states that the horizontal total derivative of vorticity is balanced by a vorticity source produced by cumulus clouds. The approximation is valid independent of the strength of cloud activities. In areas free of convective clouds, the cloud source term on the right-side of (19) vanishes. The equation is then reduced to the simple barotropic vorticity equation derived by Charney (1963) for adiabatic tropical circulations.

4. Consistency check

GATE A/B and B-scale upper air data collected during Phase III of the experiment were analyzed and used to check whether the simplified vorticity equation is consistent with the observed behavior of tropical easterly waves.

During Phase III (30 August to 18 September 1974) of GATE, a regular sequence of well developed easterly waves which originated over western Africa propagated westward across the GATE array. An excellent chronology of these waves is presented and discussed in detail by Thompson *et al.* (1979). These authors used the classification scheme first introduced by Reed and Recker (1971). Each wavelength of the easterly wave is divided into eight regions. The trough axis of the wave is designated as region 4 and the ridge axis as region 8. Regions 2 and 6 correspond to the regions of maximum northerly wind and maximum southerly wind at the 700 mb level, respectively. All other regions occupy intermediate positions. Cumulus cloud activities are usually observed to reach a maximum in or slightly ahead of the wave trough. Heavy precipitation generally occurs in regions 2 to 5.

Fig. 1 shows the time series of surface precipitation minus evaporation rates for Phase III adopted from

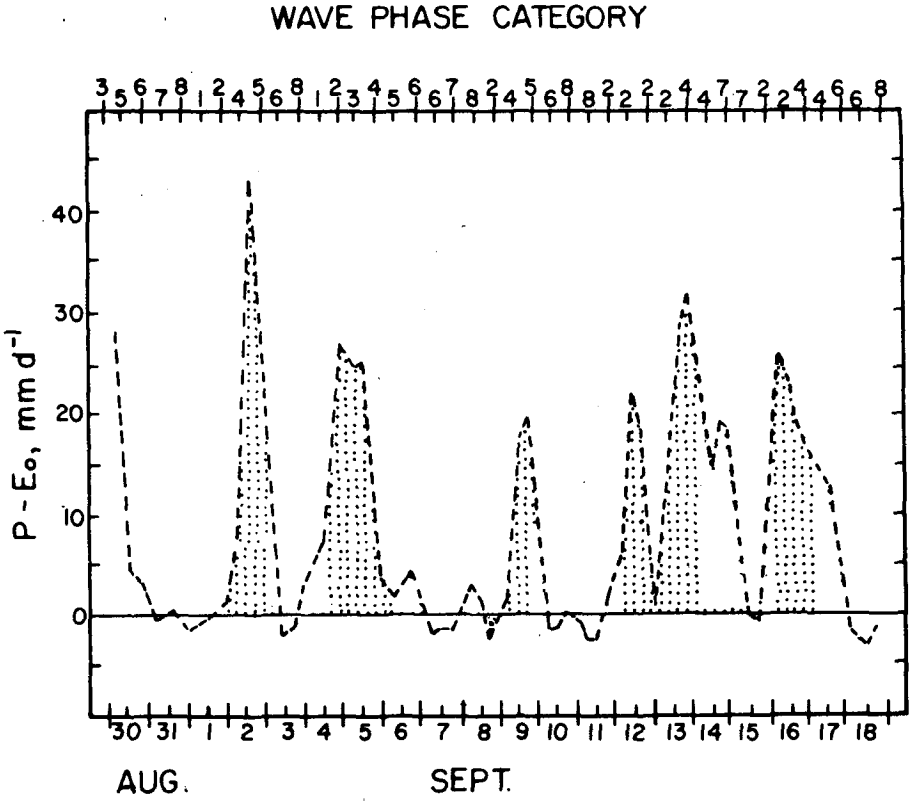

FIG. 1. The surface precipitation minus the evaporation rates for Phase III of GATE determined from B-scale ship observations. Refer to the text for explanation of wave phase category. Stippled areas indicate the periods under study.

Thompson *et al.* (1979). The precipitation rates were calculated for the B-scale area from radar measurements. The evaporation rates were determined from the bulk aerodynamic formula with a drag coefficient of 1.4×10^{-3}, using mean hourly wind and humidity measurements from the four B-scale ships: the *Dallas, Gilliss, Oceanographer* and *Researcher*. The numerals at the top of the figure are the wave phase categories at the center of the B-scale array at 1200 and 2400 GMT for each day.

The periods chosen for analysis are shown by the stippled areas in the figure. They will be identified as period 1 through 6, in chronological order. The criteria upon which the selection of the analyzed periods was made are the amount of precipitation, the strength of the mean upward vertical velocities and the wave phase category. All six periods analyzed have heavy precipitation and strong upward vertical velocities, both indications of strong convective activity. Furthermore, in order to ensure more or less similar synoptic background conditions, all periods chosen are characterized by wave regions 2 to 4.

The method of data analysis was reported in Jenkins *et al.* (1982). A detailed discussion of the heat, moisture and complete vorticity budgets for the six analyzed periods was also presented there. The purpose of that study was to compare the Cho and Cheng (1980) parameterization theory given by (17) with observations. To test the validity of the first-order vorticity equation, we simply took parts of Jenkins *et al.* (1982)'s analysis and diagnostic results as required and compared the horizontal total derivatives of vorticity with the respective cloud source terms representing the cloud life-cycle effect. The horizontal total derivative of vorticity was calculated using the analyzed A/B-scale wind and vorticity field. To compute the cloud source term on the right side of (19), the recycling rate was determined from the A/B-scale moisture budget using the diagnostic procedure introduced by Cho (1977). The mean cloud vorticity $\bar{\eta}_c$ was determined using the diagnostic method discussed in Cheng *et al.* (1980).

In Fig. 2 the vertical profiles of the observed horizontal total derivatives of vorticity (solid lines, denoted simply as $D\bar{\eta}/Dt$) and the diagnosed cloud life-cycle effects (dashed line) are compared for the six analyzed periods. The agreement is very good for periods 3, 5 and 6. Reasonably good agreement is also obtained for periods 2 and 4. Period 1 is perhaps the least satisfactory period. The diagnosed cloud life-cycle effect for this period deviates considerably from the observed horizontal total derivative of vorticity at height levels between 400 and 600 mb. When the six periods are considered as a whole, the simplified vorticity equation appears to be consistent with the observed vorticity dynamics of the easterly waves.

One of the assertions made by Cho and Cheng (1980) is the existence and importance of a horizontal eddy flux of vorticity. If the assumption is made that the horizontal eddy flux is negligible, then the parameterized apparent vorticity source is reduced to the simple form

$$Z = -M_c \frac{\partial \bar{\eta}}{\partial p} - \hat{\mathbf{k}} \cdot \nabla M_c \times \frac{\partial \bar{\mathbf{v}}}{\partial p}. \tag{20}$$

The corresponding first order vorticity equation then becomes

$$\frac{\partial \bar{\eta}}{\partial t} + \bar{\mathbf{v}} \cdot \nabla \bar{\eta} = -\bar{\eta} \nabla \cdot \bar{\mathbf{v}}, \tag{21}$$

or equivalently,

$$\frac{\partial \bar{\eta}}{\partial t} + \bar{\mathbf{v}} \cdot \nabla \bar{\eta} = -\bar{\eta} \frac{\partial M_c}{\partial p}. \tag{22}$$

In other words, when the horizontal eddy vorticity flux is negligible, the total derivative of vorticity is balanced by vortex stretching.

Fig. 3 shows the vertical profiles of the horizontal total derivative of vorticity and vortex stretching by cloud-scale convergence/divergence [corresponding to the left and right sides of (22)] for the six periods. The level of agreement appears comparable to that shown in Fig. 2, except for period 4 in which Eq. (22) gives a very poor result. The root-mean-square (rms) discrepancies between the solid and the dashed curves shown in Fig. 2, and between the solid and the dotted curves shown in Fig. 3 are computed and compared in Table 1 for the six periods. The two formulations appear to give quite comparable results. The difference in the average rms discrepancies between the two formulations is caused mainly by the poor performance of (22) in period 4.

Further support to this conclusion is obtained by noticing that when the vorticity budgets are averaged over the six periods, the two simple vorticity equations—namely (19) and (22)—give essentially the same results, as is seen in Fig. 4. The solid line in the figure shows the horizontal total derivative averaged over the six periods. The dashed and dotted lines give the averaged cloud life-cycle effect and averaged vortex stretching due to cloud-scale convergence/divergence, respectively.

One possible explanation for this result may be that all periods analyzed correspond to easterly wave regions 2–4 where maximum cloud activities are usually observed. In such regions, the horizontal eddy vorticity flux $\overline{\mathbf{v}'\eta'}$ reaches a local maximum; therefore the divergence of $\overline{\mathbf{v}'\eta'}$ becomes very small, especially when mesoscale features and individual period fluctuations are smoothed out after averaging over the six periods. Consequently, in these regions of local maximum, (19) is reduced to (22), and the two simplified equations give essentially the same result.

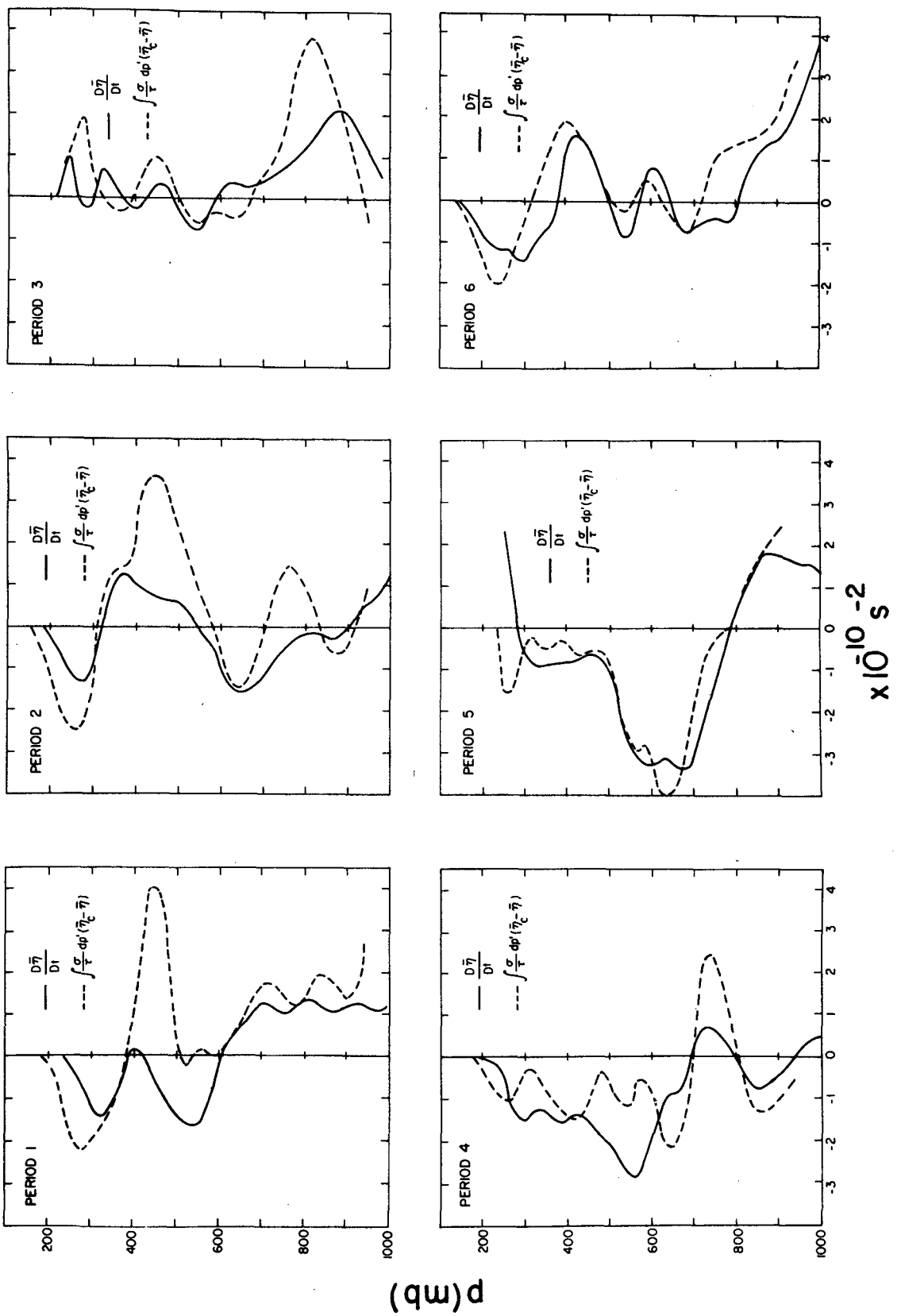

FIG. 2. Vertical profiles of the observed horizontal total derivative of vorticity (solid line) and the diagnosed cloud life-cycle effect (dashed line) for the six analyzed periods.

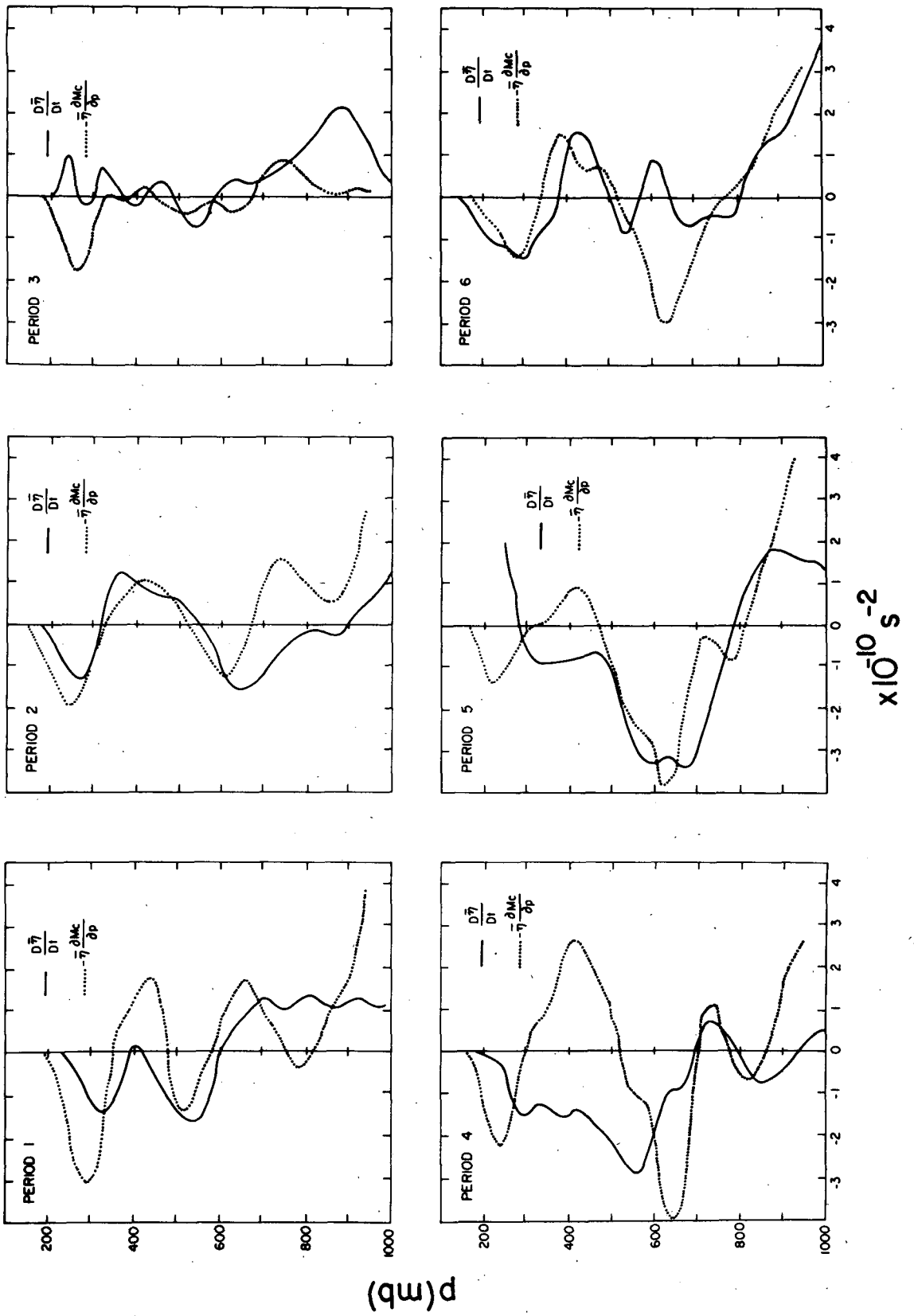

FIG. 3. Vertical profiles of the observed horizontal total derivative of vorticity (solid line) and the vortex tube stretching by cloud-scale convergence/divergence (dotted line) for the six analyzed periods.

TABLE 1. Root-mean-square values of $\left(\frac{D\bar{\eta}}{Dt} - \int \frac{\sigma}{\tau} dp'(\bar{\eta}_c - \bar{\eta})\right)$ and $\left(\frac{D\bar{\eta}}{Dt} + \bar{\eta}\frac{\partial M_c}{\partial p}\right)$ for the six analyzed periods.

Period	Root-mean-square discrepancies (10^{-10} s^{-2})	
	$\left(\frac{D\bar{\eta}}{Dt} - \int \frac{\sigma}{\tau} dp'(\bar{\eta}_c - \bar{\eta})\right)$	$\left(\frac{D\bar{\eta}}{Dt} + \bar{\eta}\frac{\partial M_c}{\partial p}\right)$
1	1.5	1.3
2	1.2	1.0
3	1.0	1.0
4	1.0	2.1
5	0.9	1.3
6	0.9	1.1
Average	1.1	1.3

5. Vorticity dynamics of tropical easterly waves observed in GATE

The first-order vorticity equation offers a simple framework in which the vorticity dynamics of tropical easterly waves may be interpreted. Assuming a steady state wave propagating with a phase velocity **c**, the vorticity equation can be written as

$$(\bar{\mathbf{V}} - \mathbf{c}) \cdot \nabla\bar{\eta} = \int \frac{\sigma}{\tau} dp'(\bar{\eta}_c - \bar{\eta}), \tag{23}$$

which states that the vorticity advection relative to the phase velocity of the wave is balanced by the generation of vorticity by cumulus clouds. The properties of such a vorticity wave may differ from those of simple barotropic Rossby waves in two aspects: first, there is a cloud source term in the governing equation, and second, due to the cloud induced convergence/divergence, the mean horizontal wind field $\bar{\mathbf{V}}$ contains both a rotational component $\bar{V}_\psi$ and an irrotational component $\bar{V}_\delta$:

$$\bar{\mathbf{V}} = \bar{\mathbf{V}}_\psi + \bar{\mathbf{V}}_\delta. \tag{24}$$

In general, the two components should be equally important. The irrotational component may be neglected only at levels where the divergence field is much weaker than the vorticity field.

Observational studies of easterly waves over the GATE area suggest that the wind field in these waves is, more or less, a rotational field in a considerably deep layer of the troposphere. Thompson *et al.* (1979) presented the composite vorticity and divergence fields of these waves in Figs. 12 and 13 of their paper. These figures show that in the layer between 900 and 400 mb, the relative vorticity is of the order of 20 $\times 10^{-6}$ s^{-1}, while the divergence is only of the order 5×10^{-6} s^{-1}. In the layer between 400 and 100 mb, both the relative vorticity and the divergence have magnitudes of the order of 10×10^{-6} s^{-1}. It appears that the wind field in the layer between 900 and 400 mb is basically a rotational field because the divergence is smaller than the relative vorticity by a factor of four. As a first order approximation, the velocity vector in this layer may therefore be expressed as

$$\bar{\mathbf{V}} = \hat{\mathbf{k}} \times \nabla\psi, \tag{25}$$

and the relative vorticity as

$$\bar{\zeta} = \nabla^2\psi, \tag{26}$$

where ψ is a streamfunction.

If we assume that the wind and vorticity fields are composed of a zonal mean state denoted by $\bar{\bar{\mathbf{V}}}$ and $\bar{\bar{\eta}}$, respectively, and a wave perturbation denoted by $\mathbf{V}''$ and η'', respectively, then

$$\bar{\mathbf{V}} = \bar{\bar{\mathbf{V}}} + \mathbf{V}'', \tag{27}$$

and

$$\bar{\eta} = \bar{\bar{\eta}} + \eta''. \tag{28}$$

Assuming that the perturbation field is a zonally propagating sinusoidal wave, η'' can be written as

$$\eta'' = \eta_0(p)e^{i(kx-\omega t+\phi)}. \tag{29}$$

Here $\eta_0(p)$ is the wave amplitude, k denotes the wave number, and ω the angular frequency. Also ϕ is a phase factor whose value is chosen in such a way that at the wave trough, $(kx - \omega t + \phi) = 2n\pi$ where n is either zero or a positive integer.

For the easterly waves observed during GATE, the total derivative of vorticity, after linearization, becomes

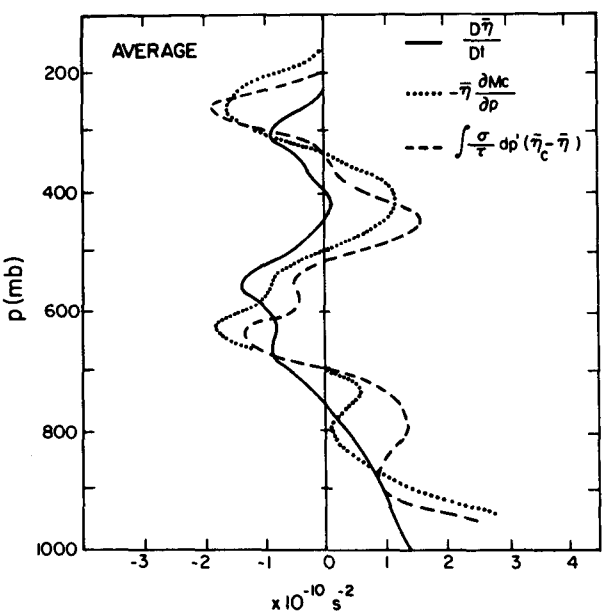

FIG. 4. Vertical profiles of the observed horizontal total derivative of vorticity (solid line), the diagnosed cloud life-cycle effect (dashed line) and the vortex tube stretching by cloud-scale convergence/divergence (dotted line), averaged over the six analyzed periods.

$$\frac{D\bar{\eta}}{Dt} = (\bar{\mathbf{V}} - \mathbf{c})\cdot\nabla\bar{\eta} = i\frac{1}{k}\left[k^2(\bar{u} - c) - \frac{\partial\bar{\eta}}{\partial y}\right]\eta''(p) \quad (30)$$

within the layer between 900 and 400 mb where the wind field is approximately rotational. Here $c = \omega/k$ is the phase speed. The advection of vorticity relative to the wave speed has two components corresponding to the two terms in the square bracket: the advection of the wave vorticity by the mean zonal wind and of the zonal mean vorticity by the wave-induced meridional wind.

Also implicit in (29) is the assumption that the wave has no north–south structure. This is of course not a realistic assumption. However, it will not affect our analysis if (29) is applied only along the main east–west axis of the wave. Along this axis, the relative wave vorticity is a maximum in the meridional direction. Therefore the advection of wave vorticity in the north–south direction should be negligible.

The meridional distribution of the zonal mean vorticity over the eastern Atlantic region during Phase III of GATE was presented by Reed *et al.* (1977). From their diagram, the $\partial\bar{\eta}/\partial y$ over the GATE area can be estimated. The vertical profile of mean zonal wind $\bar{u}$ during Phase III of GATE was presented by Thompson *et al.* Their Fig. 3 shows that relative to an average propagation speed of 8 m s^{-1} for the easterly waves, the mean zonal wind is directed eastward below 250 mb and westward between 150 and 250 mb. Due to the presence of the west African easterly jet, there is a local minimum in the relative eastward wind at the 650 mb level.

The relative magnitudes of the two components of

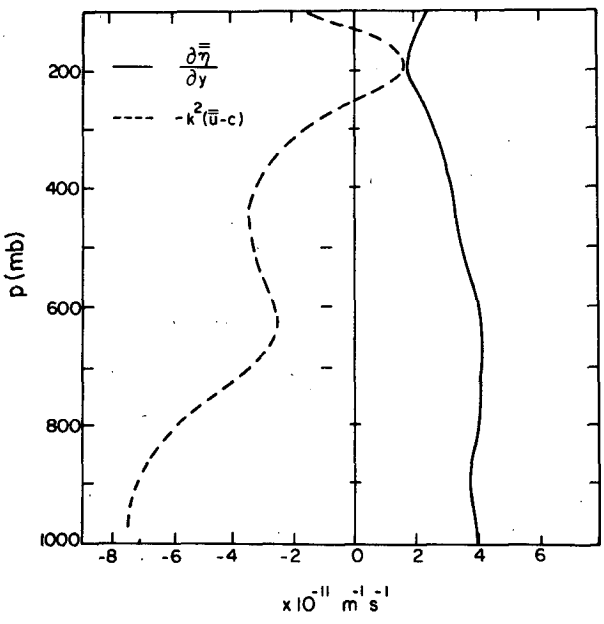

FIG. 5. Vertical profiles of $\partial\bar{\eta}/\partial y$ (solid line) and $-k^2(\bar{u} - c)$ (dashed line).

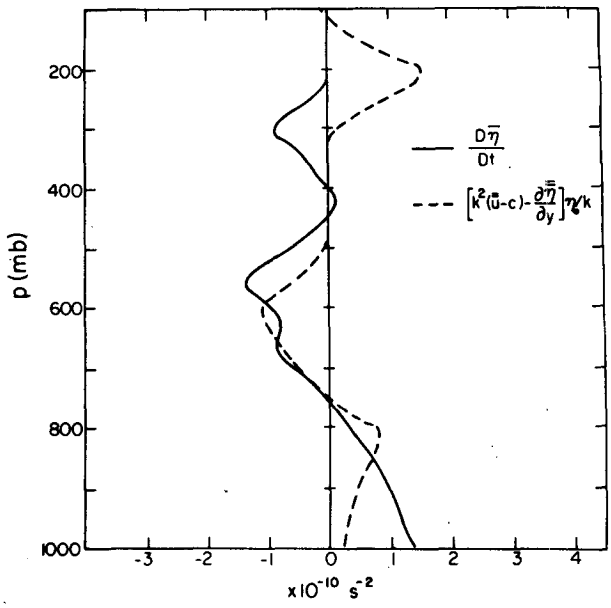

FIG. 6. Vertical profiles of the observed horizontal total derivative of vorticity averaged over the six analyzed periods (solid line) and the total derivative of vorticity for a sinusoidal non-divergent vorticity wave (dashed line).

vorticity advection in the easterly waves are shown in Fig. 5. It was assumed in the calculations that $c = -8$ m s^{-1} and $k = 2\pi\lambda^{-1}$ with $\lambda = 2500$ km. The term $\partial\bar{\eta}/\partial y$ (solid line) is positive throughout the entire troposphere, indicating a northward increase of the zonal mean absolute vorticity. The advection of wave vorticity by the mean zonal wind (dashed line) and the advection of zonal mean vorticity by the wave-induced meridional wind (solid line) are opposite in sign below 300 mb. This indicates that, except for the presence of the cloud forcing, the evolution of the vorticity field below 300 mb is somewhat similar to that of a simple Rossby wave. In the layer between 150 and 300 mb, the two components of the vorticity advection are of the same sign. The evolution of vorticity field in this layer must be entirely different from the behavior of barotropic Rossby waves. As mentioned earlier, at these levels the irrotational wind component is no longer negligible; advection of vorticity by the divergent wind at these levels must be very important. Also note that the advection of the wave vorticity by the mean zonal wind has a local minimum at the 650 mb level. This is, of course, due to the presence of the easterly jet at that level.

To check how well the vorticity advection processes are represented by the simple wave calculations, we compare in Fig. 6 the observed horizontal total derivative of vorticity averaged over the six analyzed periods (solid line) to the total derivative of vorticity for a sinusoidal non-divergent vorticity wave (dashed line). In obtaining the vertical profile, the

vertical distribution of vorticity at the trough region of the Thompson *et al.* composite easterly wave is used as the amplitude $\eta_0(p)$ of the wave. The figure shows that the observed total derivative of vorticity is fairly well represented by the simple vorticity-wave calculation in the layer between 900 and 400 mb. Or, in other words, provided that the cloud forcing is taken into consideration, easterly waves observed over the eastern Atlantic are Rossby-type waves in the layer between 900 and 400 mb. Above 400 mb, where cumulus clouds induce very strong divergence, the vorticity advection by the irrotational wind component becomes important in the evolution of the vorticity field. Below 900 mb, both the irrotational wind and microscale turbulent diffusion are important effects.

One curious feature in the Thompson *et al.* composite easterly wave is the presence of a layer of pronounced mid-level divergence centered around 600 mb over wave regions 2–4, with a maximum located over wave region 3. It is of interest to note that this feature is located at the level of the west African easterly jet. Its presence is consistent with the vorticity dynamics described by the first-order vorticity equation.

As discussed in the previous section, cumulus cloud activities usually reach a maximum over wave regions 2–4. In these regions, after mesoscale features are smoothed out, the divergence of the horizontal eddy vorticity flux becomes negligible. Consequently, comparing (19) and (22), the cloud forcing term represented by the cloud life-cycle effect may be written as

$$\int \frac{\sigma}{\tau}\, dp'(\bar{\eta}_c - \bar{\eta}) = -\bar{\eta}\frac{\partial M_c}{\partial p}. \tag{31}$$

The first order vorticity equation over, say, wave region 3 may be written as

$$(\bar{\mathbf{V}} - \mathbf{c})\cdot\nabla\bar{\eta} = -\bar{\eta}\frac{\partial M_c}{\partial p}. \tag{32}$$

Without implying any cause-effect relationship, levels of horizontal convergence or divergence of the total cloud mass flux correspond to levels of negative or positive advection of vorticity relative to the propagation velocity of the wave. Due to the presence of the easterly jet centered at 650 mb, the negative advection of wave vorticity by the mean zonal wind reaches a minimum at that level, as can be seen in the dashed curve in Fig. 6. Consequently, the net vorticity advection around 600 mb becomes positive. Eq. (32) then implies that at this level there should be a net horizontal divergence of cloud mass flux, which is reflected on the synoptic scale as the divergence of the mean wind field. Therefore, it appears that the pronounced mid-level divergence often observed in GATE during convectively-active periods is associated with the vorticity advection by the west African easterly jet.

6. Concluding remarks

We present, in this paper, the derivation of a first-order vorticity equation for tropical disturbances. The equation indicates that the evolution of the vorticity field in the tropics is caused mainly by the horizontal advection of vorticity, and a vorticity source represented by the cloud life-cycle effect. The physical basis for this equation can be summarized as follows.

The synoptic-scale mean vorticity is essentially equal to the mean vorticity of the cloud environment so long as the fractional area occupied by cumulus clouds is of the order of 10% or less. This was proved by Cho *et al.* (1979) and Cho and Cheng (1980). The evolution of the synoptic-scale mean vorticity field must therefore be the same as that of the mean cloud environmental vorticity.

The vorticity field in the cloud environment is influenced by the cloud environmental flow. The vertical advection, tilting and stretching of vorticity in the cloud environment are not very important because the vertical motion in the cloud environment is very weak. Therefore, the horizontal advection of vorticity is the only important process within the cloud environment.

Deviations from the environmental mean vorticity are induced inside areas occupied by clouds by processes at the cloud scale. At the end of the active periods of the clouds, areas occupied by clouds become part of the cloud environment. The excessive vorticity in these cloud areas then becomes part of the cloud environmental vorticity. This is the cloud life-cycle effect discussed by Cho (1977). It represents a source for the cloud environmental vorticity field. Thus, in addition to the horizontal advection, the evolution of the mean cloud environmental vorticity is also affected by the cloud life-cycle effect. This is the essence of the first-order vorticity equation derived formally in Section 3.

The A/B-scale vorticity budgets for Phase III of GATE were analyzed to check whether the derived first order vorticity equation is consistent with the observed behavior of the vorticity field. The consistency check, however, should not be considered a complete verification of the theoretical derivation. Since the cloud source term used in the analysis is diagnosed from observational data, the consistency check affords only a corroboration between theory and observation. The good agreement between the theory and observations provides merely additional confidence in our theoretical development.

In addition to diagnostic studies, the proposed first-order vorticity equation must also be tested through prognostic applications of the equation. However, before the equation can be used for prognostic pur-

poses we need to resolve first the closure problem. We need to know the spectrum and amount of clouds for any given set of synoptic-scale conditions in order to simulate the evolution of the vorticity field.

Also, we should note that the first-order vorticity equation and the thermodynamic equation do not form a complete set of first order equations for tropical disturbances. In order to predict the temperature field, the vertical velocity field in the cloud environment $\tilde{\omega}$, which is usually a small difference between two large quantities, $\tilde{\omega}$ and $\bar{M}_c$, is required. How to determine this vertical motion field in the cloud environment is one of the important remaining problems in our attempts to understand the dynamics of the tropical atmosphere.

Acknowledgments. This work was supported by research grants from the Canadian National Science and Engineering Research Council and the Atmospheric Environment Service of Canada. The authors wish to thank Professor R. J. Reed for many useful discussions, and two anonymous reviewers for helpful suggestions. This manuscript was typed by Janet Cooper and Margaret Currie.

REFERENCES

Arakawa, A., and W. H. Schubert, 1974: Interaction of a cumulus cloud ensemble with the large-scale environment. Part I. *J. Atmos. Sci.*, **31,** 674–701.

Charney, J. G., 1963: A note on large-scale motions in the tropics. *J. Atmos. Sci.*, **20,** 607–609.

Cheng, L., T. C. Yip and H. R. Cho, 1980: Determination of mean cumulus cloud vorticity from GATE A/B-scale potential vorticity budget. *J. Atmos. Sci.*, **37,** 797–811.

Cho, H. R., 1977: Contribution of cumulus cloud life-cycle effects to the large-scale heat and moisture budget equations. *J. Atmos. Sci.*, **34,** 87–97.

——, and L. Cheng, 1980: Parameterization of horizontal transport of vorticity by cumulus convection. *J. Atmos. Sci.*, **37,** 812–826.

——, —— and R. M. Bloxam, 1979: The representation of cumulus cloud effects in the large-scale vorticity equation. *J. Atmos. Sci.*, **36,** 127–139.

Chu, J. H., M. Yanai and C. H. Sui, 1981: Effects of cumulus convection on the vorticity field in the tropics. Part I: The large-scale budget. *J. Meteor. Soc. Japan,* **59,** 535–546.

Fraedrich, K., 1973: On the parameterization of cumulus convection by lateral mixing and compensating subsidence. Part I. *J. Atmos. Sci.*, **30,** 408–413.

Jenkins, M. A., R. M. Bloxam and H. R. Cho, 1982: Further test of a theory of convective effects on the large-scale vorticity field in the tropics. *Atmos. Ocean,* **20,** 207–226.

Johnson, R. H., 1976: The role of convective-scale precipitation-downdrafts in cumulus and synoptic-scale interactions. *J. Atmos. Sci.*, **33,** 1890–1910.

Nitta, T., 1975: Observational determination of cloud mass flux distributions. *J. Atmos. Sci.*, **32,** 73–91.

Ooyama, K., 1971: A theory on parameterization of cumulus convection. *J. Meteor. Soc. Japan,* **49,** 744–756.

Reed, R. J., and E. E. Recker, 1971: Structure and properties of synoptic-scale wave disturbances in the equatorial western Pacific. *J. Atmos. Sci.*, **28,** 1117–1133.

——, D. C. Norquist and E. E. Recker, 1977: The structure and properties of African wave disturbances as observed during Phase III of GATE. *Mon. Wea. Rev.*, **105,** 317–333.

Shapiro, L. J., 1978: The vorticity budget of a composite African tropical wave disturbance. *Mon. Wea. Rev.*, **106,** 806–817.

——, and D. E. Stevens, 1980: Parameterization of convective effects on the momentum and vorticity budgets of synoptic-scale Atlantic tropical waves. *Mon. Wea. Rev.*, **108,** 1816–1826.

Thompson, R. M., S. W. Payne, E. E. Recker and R. J. Reed, 1979: Structure and properties of synoptic-scale wave disturbances in the Intertropical Convergence Zone of the eastern Atlantic. *J. Atmos. Sci.*, **36,** 53–72.

Wallace, J. M., 1971: Spectral studies of tropospheric wave disturbances in the tropical western Pacific. *Rev. Geophys. Space Phys.*, **9,** 557–612.

Yanai, M., S. Esbensen and J. H. Chu, 1973: Determination of bulk properties of tropical cloud clusters from large-scale heat and moisture budgets. *J. Atmos. Sci.*, **30,** 611–627.

——, C. H. Sui and J. H. Chu, 1982: Effects of cumulus convection on the vorticity field in the tropics. Part II: Interpretation. *J. Meteor. Soc. Japan,* **60,** 411–423.